

Specific heat of Sb: Isotopic and spin-orbit effects from measurements and *ab initio* calculations

J. Serrano,^{1,2,*} R. K. Kremer,³ M. Cardona,³ G. Siegle,³ L. E. Díaz-Sánchez,^{4,5} and A. H. Romero⁴

¹European Synchrotron Radiation Facility, Boite Postale 220, 38043 Grenoble, France

²ICREA and Department of Applied Physics, Universitat Politècnica de Catalunya, EPSC, Av. Canal Olímpic 15, E-08860 Castelldefels, Spain

³Max Planck Institut für Festkörperforschung, Heisenbergstrasse 1, D-70569 Stuttgart, Germany

⁴CINVESTAV, Departamento de Materiales, Unidad Querétaro, Querétaro 76230, Mexico

⁵Unité de Physico-Chimie et Physique des Matériaux, Université Catholique de Louvain, B-1348 Louvaine-la-Neuve, Belgium

(Received 27 November 2007; published 25 February 2008)

We report measurements of the specific heat C of antimony crystals in the 2–50 K temperature range for several isotopic compositions and *ab initio* calculations of the specific heat as a function of temperature. The contribution of spin-orbit interaction and the dependence of C on isotopic mass are discussed and compared with previous observations reported for semiconductors and group VA semimetals. We also discuss the effect of spin-orbit interaction on the trigonal lattice parameter and the cohesive energy.

DOI: [10.1103/PhysRevB.77.054303](https://doi.org/10.1103/PhysRevB.77.054303)

PACS number(s): 65.40.Ba, 63.20.D-, 71.70.Ej, 31.15.A-

I. INTRODUCTION

In the last years, a number of publications have reported the temperature dependence of the specific heat C in monatomic^{1–3} and binary^{4–6} semiconductors as a function of the isotopic mass of its constituent atoms. Some general trends were observed in all investigated materials, namely, (i) a peak appears at low temperature T in the plot of C/T^3 vs T , (ii) this peak is higher for larger isotopic masses M , and (iii) in monatomic crystals, there is a unique relation between the temperature dependence of $d \ln(C/T^3)/d \ln M$ and that of $d \ln(C/T^3)/d \ln T$. This relation carries over to binary semiconductors if one considers the sum of the logarithmic derivatives with respect to the isotopic masses. These trends were reproduced by first-principles calculations based on the linear response method and density functional perturbation theory. Contrary to this, little information is available on the thermodynamic properties of semimetals, in particular, the specific heat, where both electronic and lattice degrees of freedom play a role. With the exception of phosphorus, the group of the VA elements exhibit the A7 rhombohedral structure (space group $R\bar{3}m$, No. 166 in the International Crystallographic Tables). This structure is generated by applying a deformation along the threefold axis to an fcc lattice plus a relative displacement of atoms, which results into a primitive cell with two atoms.⁷ Among these elements, antimony is known for the strongly anharmonic behavior of the crystal lattice, as revealed by the Raman-Brillouin scattering, in particular, under pressure.^{8,9} The anharmonicity, together with the semimetallic character of their electronic structure and, for heavier elements, the increasing importance of spin-orbit interaction, has hindered so far an accurate investigation of their thermodynamic and lattice dynamical properties by means of *ab initio* calculations. For example, only very recently, spin-orbit interaction has been taken into account for calculations of these properties in bismuth.^{10–12}

From the experimental point of view, there are only a few works going back to the 1960s, dealing with the specific heat of arsenic,^{13–15} antimony,^{16–18} and bismuth.^{19,20} Due to the limitations of the experimental equipment, the reported data

show considerable scattering in the 5–20 K temperature region. It is precisely in this temperature range where the most interesting effects occur, i.e., the described trends seen for semiconductors and the deviation from the Debye behavior, as well as the presence of both electronic and lattice contributions.

In this paper, we report specific heat measurements of antimony crystals in the 2–50 K temperature range both for natural samples as well as isotopically enriched ¹²¹Sb and ¹²³Sb. The experimental data are compared with *ab initio* simulations of the lattice dynamics and the specific heat. These simulations were performed with a relativistic pseudo-potential Hamiltonian that includes the spin-orbit interaction. The effect of spin-orbit interaction is expected to be important although not as large as recently reported for bismuth.¹¹

Concerning the dependence on isotope mass, we found analogous behavior as that for monatomic semiconductors. Additionally, we have calculated the effect of spin-orbit interaction on the trigonal lattice parameter and the cohesive energy. Like in the case of bismuth,¹¹ we found the effects of spin-orbit interaction to be approximately quadratic on the spin-orbit coupling parameter, a linear term being absent.

II. EXPERIMENTAL METHOD

Natural samples of antimony were obtained from the Preussag Pure Metals (Langelsheim, Germany). They consisted of small single crystals of a purity of 99.9999%. Isotopically enriched ¹²¹Sb and ¹²³Sb with 99% isotope abundance in either case were purchased from the Oak Ridge National Laboratory. According to their assay, the chemical purity of both enriched isotopes was better than 5×10^{-4} . They appeared to be, upon microscope observation, single crystals of about 2 mm³ size. Pieces of the three isotope modifications, weighing about 30 mg, were used as purchased for the specific heat measurements, without any additional treatment. For details about the calorimeter and the experimental procedure, see Refs. 2–4. The measurements were performed under vacuum, i.e., at constant pressure. We do not distinguish here between the specific heat obtained at

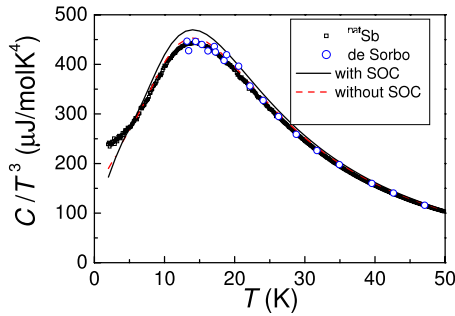


FIG. 1. (Color online) Temperature dependence of the specific heat of natural antimony. The experimental data (open squares) are compared with data from the literature Ref. 16 (solid circles) and with *ab initio* calculations with (black, solid) and without (red, dashed) spin-orbit interactions.

constant volume or constant (zero) pressure since, in the temperature region under consideration, they coincide within error.^{4,6}

III. AB INITIO CALCULATIONS

First-principles methods have proved to be essential to identify the phonon modes responsible for the temperature dependence of the specific heat in semiconductors. In this work, we report *ab initio* calculations of the specific heat of antimony and the lattice dynamics obtained with the ABINIT software package.^{21,24,25}

The electronic structure of antimony in the $R\bar{3}m$ phase was calculated using the Hartwigsen-Goedecker-Hutter pseudopotentials which are expressed as norm-conserving separable dual space Gaussians and generated on the basis of a fully relativistic all-electron calculation.²² To this aim, a grid of $12 \times 12 \times 12$ k -points in the Brillouin zone was used for the integration required for the determination of the local charge density. The local density approximation to the exchange and correlation energy was employed.²⁶

The dynamical matrices corresponding to a grid of $12 \times 12 \times 12$ q points were calculated within the framework of density functional perturbation theory and the linear response method. These matrices were then interpolated to obtain, by integration, the lattice contribution to the specific heat at constant volume.^{23–25} Details of the procedure and equations to calculate this contribution have been reported elsewhere.⁵

The implementation of the spin-orbit term in ABINIT follows the same lines as in Ref. 27, where the spin-orbit term in the Hamiltonian is applied only into the Kleinmann-Bylander type of nonlocal operator. For the electronic calculations, the spin-orbit Hamiltonian was multiplied by a parameter λ . Thus, $\lambda=0$ corresponded to neglecting the spin-orbit coupling, whereas for $\lambda=+1$, the full spin-orbit coupling was applied. We also performed calculations for $\lambda=0.5$ and $\lambda=-1$, so as to confirm the quadratic dependence of thermodynamic properties on λ proposed in Ref. 11.

IV. DISCUSSION

Figure 1 displays the temperature dependence of C/T^3

measured for natural antimony (open squares) together with data previously reported in Ref. 16 (open circles). Our measurements provide a much clearer description of the behavior at temperatures lower than 15 K, whereas at higher temperatures, both data sets are basically indistinguishable.

In a semimetal, the low temperature limit of the specific heat can be described by the equation

$$C = \gamma T + \beta T^3 + \alpha T^{-2}, \quad (1)$$

where the linear term represents the electronic contribution, the cubic term corresponds to the Debye behavior of the crystal lattice, and the T^{-2} term describes the interaction of the nuclear quadrupole moment with the electric field gradient of the electrons and the lattice. The latter term is negligible within our temperature range, but it may become appreciable for $T < 1$ K. The upward bending at low temperatures (cf. Fig. 1) is due to the electronic contribution (γ) to the specific heat.¹⁷ A fit of the low temperature heat capacities with Eq. (1) gives $\gamma=0.13(4)$ mJ mol⁻¹ K⁻² and $\beta=0.234(2)$ mJ mol⁻¹ K⁻⁴ ($\alpha=0$). These values are nearly independent of the isotope composition and in good agreement with those reported in Refs. 14 and 17.

The peak in Fig. 1, located at 14 K, evidences the deviation from the Debye behavior that is known to occur at low temperatures. Within the Einstein model, this peak should correspond to a phonon frequency of 7 meV,⁶ which coincides with the first maximum of the calculated phonon density of states, i.e., it corresponds to transverse acoustic modes.²⁸

Figure 1 also displays the calculated temperature dependence of the specific heat with (black, solid) and without (red, dashed) the spin-orbit interaction. Both calculations reproduce well the temperature dependence and the peak position in the experimental data. The spin-orbit interaction produces an enhancement of the peak of C/T^3 by $\sim 4\%$. Very recently, the contribution of spin-orbit interaction to the specific heat of bismuth was reported to be quadratic in λ at low values of λ .¹¹ For $0.5 < \lambda < 1$, a cubic term becomes important, but no linear term in λ is observed. Considering that the spin-orbit splitting of bismuth (1.7 eV) is 2.42 times that of antimony (0.7 eV),²⁹ if we take the value for $\lambda=1/2.42=0.41$ in Eq. (1) of Ref. 11, we expect an increase of 2.4% for the peak of C/T^3 for antimony, in qualitative agreement with our direct calculations. The difference between 2.4% and 4% might be related to the role of cubic terms in λ , neglected in Eq. (1) of Ref. 11. Both in bismuth¹¹ and antimony, there is a 5% discrepancy between the calculations (including spin-orbit interaction) and experimental results. This discrepancy might be related to the intrinsic inaccuracy of local density approximation phonon dispersions, as compared to the experimental values.

Figure 2 displays the dependence of the peak of C/T^3 on isotope mass. For the sake of comparison, the linear temperature term has been subtracted from the experimental data, since it is not taken into account in the calculations. The curves of Fig. 2 show an increase of the peak with increasing isotope mass, both for the experimental and calculated data. This trend, already reported for semiconductors in previous works,^{2,4–6} seems also to be obeyed by semimetals. The iso-

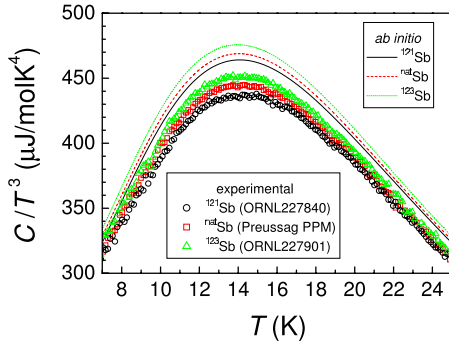


FIG. 2. (Color online) Same as Fig. 1 for different isotope compositions. The calculations were performed in all cases including spin-orbit interactions ($\lambda=+1$).

tope shift of the peak between ^{121}Sb and ^{123}Sb amounts to $12 \mu\text{J mol}^{-1} \text{K}^{-4}$ and agrees reasonably well with the experimental shift, $14.2 \mu\text{J mol}^{-1} \text{K}^{-4}$. The calculated curve corresponding to antimony with natural isotope composition is slightly closer to that of ^{121}Sb due to the closer masses. In the case of experimental data, we found that this rather subtle effect depends somewhat on the sample details.

Figure 3 displays (full circles) the logarithmic derivative of C/T^3 with respect to the isotope mass corresponding to the experimental data obtained after subtraction of the electronic contribution [γ term in Eq. (1)]. This derivative has been reported to be linked to the logarithmic derivative with respect to temperature in diamond, silicon, and germanium by¹

$$\frac{d \ln(C/T^3)}{d \ln M} = \frac{1}{2} \left[3 + \frac{d \ln(C/T^3)}{d \ln T} \right]. \quad (2)$$

We show in Fig. 3 the left- and right-hand sides (rhs) of Eq. (2) obtained from the experimental data with full (red) and open (black) circles, respectively, and the rhs of Eq. (2) calculated from the *ab initio* data for $\lambda=+1$ (solid line). The agreement between both experimental data sets, as well as the agreement with the *ab initio* data, is excellent. The good

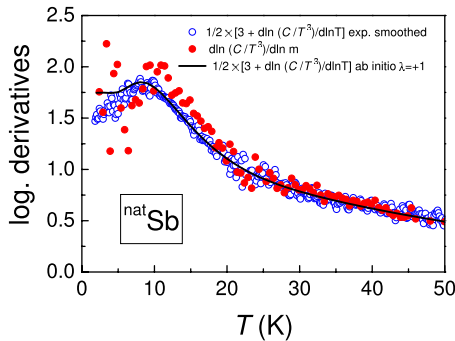


FIG. 3. (Color online) Logarithmic derivative with respect to the isotope mass, $d \ln(C/T^3)/d \ln M$ (solid red circles) and rhs of Eq. (2) (open black circles), corresponding to the experimental data. The solid line displays the rhs of Eq. (2) obtained from the calculations.

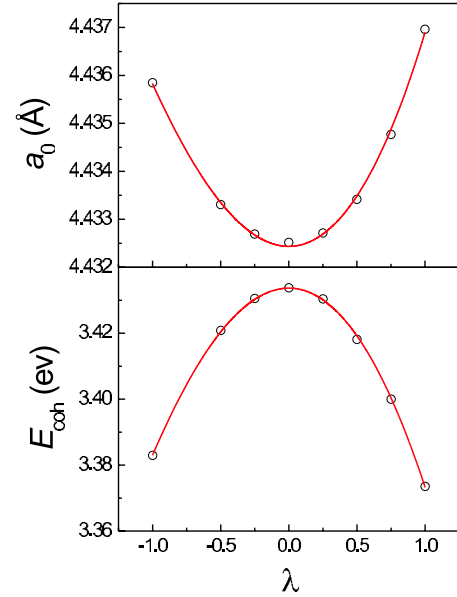


FIG. 4. (Color online) Dependence of the lattice parameter a_0 and the cohesive energy E_{coh} on the strength of the spin-orbit interaction. The solid line displays a fit with a polynomial of third order, $y(\lambda)=y_0(0)[1+c_2\lambda^2(1+c_3\lambda)]$ ($y=a_0, E_{coh}$), with $a_0=4.43244(4)$, $c_2=0.00089(2)$, and $c_3=0.136(13)$ and $E_0=3.4337(3)$ Å, $c_2=-0.0162(2)$, and $c_3=0.088(7)$ for the lattice parameter a_0 and the cohesive energy E_{coh} , respectively (see Discussion in Sec. IV).

agreement between both sets allows us to verify the validity of this equation for semimetals. The peak at 10 K is followed by two different slopes at higher temperatures, the crossover point being at ~ 25 K. The associated phonon frequency is 11.5 meV, calculated again by multiplying the crossover temperature by a factor of 6.⁶ This frequency corresponds to the threshold between acoustic and optic phonons, as shown in the phonon dispersion relations obtained by inelastic neutron scattering experiments²⁸ and confirmed by our calculations.³⁰ Hence, we attribute the change in slope to the activation of optic phonons at higher temperatures.

In recent works on bismuth,^{10,11} a significant contribution of spin-orbit interaction to vibrational properties such as phonon dispersion relations and specific heat has been found. The relevance of these effects can be evaluated by performing *ab initio* simulations of the properties of interest as a function of the magnitude of the spin-orbit interaction, governed by the coupling parameter λ . Figure 4 displays the change in the trigonal lattice constant a_0 and the cohesive energy E_{coh} as a function of λ . The calculated data show a quasiparabolic dependence on λ , with a small but nevertheless significant contribution of a cubic term. The experimental value of $E_{coh}=2.7$ eV compares well with the calculated value for $\lambda=+1$, i.e., 3.37 eV. A similar agreement was reported in Ref. 11 for bismuth. The expansion of the spin-orbit Hamiltonian in λ using perturbation theory contains only quadratic and higher order terms in λ , since linear terms in λ would imply a splitting between z components of the spin upon the spin-orbit interaction, a splitting that can only happen in the presence of a magnetic field. Therefore, no linear term in the dependence of both a_0 and E_{coh} on λ is

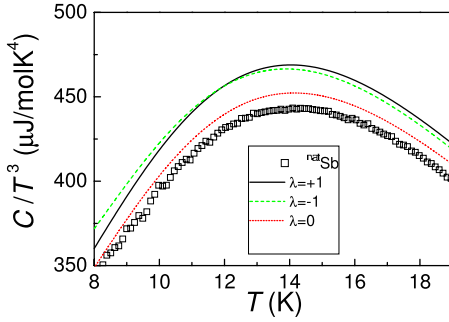


FIG. 5. (Color online) Dependence of the peak C/T^3 on the strength of the spin-orbit interaction. The symbols display our experimental data for the natural isotope composition, whereas the curves display the results of the calculations for $\lambda=+1$ (black, solid), $\lambda=0$ (red, dotted), and $\lambda=-1$ (green, dashed).

expected. Note that the square root of the ratio of the coefficients corresponding to the quadratic term in λ for the fits of a_0 of bismuth¹¹ and antimony, which amounts to 2.75, is rather similar to that of the spin-orbit splittings, i.e., $1.7/0.7=2.42$.²⁹ The difference between 2.75 and 2.42 may be due to the fact that the corresponding energy denominators are smaller in Bi than in Sb. A similar comparison can be effected for the cubic root of the ratio of the cubic terms which for a_0 turns out to be 2.8, close to the ratio of spin-orbit splittings. This relation, which also holds for the dependence of the peak C/T^3 on λ , implies a simple scaling of the effects of spin-orbit interaction on the vibrational properties.

Figure 5 displays the change of the specific heat with λ as a function of temperature. Two main effects are observed, namely, a larger value of the peak C/T^3 with increasing strength of the spin-orbit interaction and a crossing of the curves corresponding to $\lambda=+1$ and $\lambda=-1$. The observed

crossing suggests a change in the slope of the phonon dispersion corresponding to low frequency acoustic modes, since a shift of the peak to lower temperatures is caused by an increase of the lowest phonon frequencies. The phonon dispersion data reported for bismuth in Table II of Ref. 12 manifest a change of slope of transverse acoustic [$A(E_g)$] modes along the Γ - T direction between $\lambda=0$ and $\lambda=1$, i.e., an indication of a crossing of the dispersion relations also for bismuth (unfortunately, no calculations for $\lambda=-1$ were reported in Ref. 12). Table I displays the acoustic phonon frequencies of antimony along the Γ - T direction calculated for $\lambda=0, 1$, and -1 . A higher sound speed is observed in the case of $A(E_g)$ modes for $\lambda=1$ and -1 , as compared to that obtained without spin-orbit interaction. On the contrary, the same phonon branch shows higher frequencies for $\lambda=0$ close to the zone boundary, thus evidencing a crossing of the $A(E_g)$ bands similar to that just mentioned for Bi. Table I also displays a crossing of the $\lambda=+1$ and the $\lambda=-1$ bands.

In conclusion, we have reported measurements of the dependence of the specific heat of antimony on the isotope mass as a function temperature. The experimental data have been analyzed with the aid of first-principles calculations of the lattice dynamics and its contribution to the specific heat. The specific heat of antimony shows a similar behavior with changing isotope mass as observed in semiconductors, namely, a peak of C/T^3 vs T whose strength increases with the isotope mass, and a relation between the logarithmic derivatives with respect to isotope mass and temperature. Moreover, the *ab initio* calculations allowed us to evaluate the contribution of the spin-orbit interaction to the specific heat, the lattice parameter, and the cohesive energy. These three physical quantities depend nearly quadratically on the spin-orbit coupling parameter λ , with a minor contribution of a cubic term. The quadratic dependence is proportional to the square root of the spin-orbit splitting, as evidenced in the comparison of results for bismuth and antimony.

TABLE I. Phonon frequencies (meV) along the Γ - T direction, calculated for Sb, corresponding to transverse [$A(E_g)$] and longitudinal [$A(A_{1g})$] acoustic modes. Experimental values from Ref. 28.

	Expt.		$\lambda=0$		$\lambda=+1$		$\lambda=-1$	
	$A(E_g)$	$A(A_{1g})$	$A(E_g)$	$A(A_{1g})$	$A(E_g)$	$A(A_{1g})$	$A(E_g)$	$A(A_{1g})$
Γ			0.00	0.00	0.00	0.00	0.00	0.00
0.1	1.2		1.31	1.67	1.33	1.61	1.32	1.64
0.2	2.7		2.61	3.16	2.55	3.13	2.59	3.20
0.3	4.0		3.73	4.55	3.65	4.48	3.69	4.53
0.4	4.8	5.4	4.72	5.94	4.63	5.85	4.68	5.91
0.5	5.6	6.6	5.67	7.23	5.51	7.07	5.58	7.13
0.6	6.5	7.7	6.47	8.36	6.33	8.22	6.41	8.31
0.7	7.0	8.4	7.21	9.37	7.04	9.23	7.13	9.30
0.8	7.4	9.1	7.70	10.09	7.52	9.94	7.65	10.07
0.9	7.7	9.5	8.04	10.62	7.84	10.45	7.97	10.57
T	7.8	9.6	8.26	10.76	8.04	10.62	8.17	10.74

ACKNOWLEDGMENTS

We acknowledge very fruitful discussions with X. Gonze and thank K. Syassen and M. Krisch for a critical reading of the paper. A.H.R. and L.E.D.-S. acknowledge financial sup-

port from CONACYT under Grant Nos. J-59853-F and 167176. We also thank the CNS of IPICYT in Mexico and high power computing resources at UCL for allocation of computing time.

*jserrano@fa.upc.edu

- ¹M. Sanati, S. K. Estreicher, and M. Cardona, *Solid State Commun.* **131**, 229 (2004).
- ²M. Cardona, R. K. Kremer, M. Sanati, S. K. Estreicher, and T. R. Anthony, *Solid State Commun.* **133**, 465 (2005).
- ³A. Gibin, G. G. Devyatikh, A. V. Gusev, R. K. Kremer, M. Cardona, and H. Pohl, *Solid State Commun.* **133**, 569 (2005).
- ⁴R. K. Kremer, M. Cardona, E. Schmitt, J. Blumm, S. K. Estreicher, M. Sanati, M. Bockowski, I. Grzegory, T. Suski, and A. Jezowski, *Phys. Rev. B* **72**, 075209 (2005).
- ⁵J. Serrano, R. K. Kremer, M. Cardona, G. Siegle, A. H. Romero, and R. Lauck, *Phys. Rev. B* **73**, 094303 (2006).
- ⁶M. Cardona, R. K. Kremer, R. Lauck, G. Siegle, J. Serrano, and A. H. Romero, *Phys. Rev. B* **76**, 075211 (2007).
- ⁷J. Donohue, *The Structures of the Elements* (Wiley, New York, 1974).
- ⁸X. Wang, K. Kunc, I. Loa, U. Schwarz, and K. Syassen, *Phys. Rev. B* **74**, 134305 (2006).
- ⁹G. A. Saunders and Y. K. Yöğnurtçu, *Phys. Rev. B* **30**, 5734 (1984).
- ¹⁰É. D. Murray, S. Fahy, D. Prendergast, T. Ogitsu, D. M. Fritz, and D. A. Reis, *Phys. Rev. B* **75**, 184301 (2007).
- ¹¹L. E. Díaz-Sánchez, A. H. Romero, M. Cardona, R. K. Kremer, and X. Gonze, *Phys. Rev. Lett.* **99**, 165504 (2007).
- ¹²L. E. Díaz-Sánchez, A. H. Romero, and X. Gonze, *Phys. Rev. B* **76**, 104302 (2007).
- ¹³V. V. Nogteva, I. E. Paukov, and P. G. Strelkov, *Sov. Phys. Solid State* **7**, 1884 (1966).
- ¹⁴H. V. Culbert, *Phys. Rev.* **157**, 560 (1967).
- ¹⁵W. A. Taylor, D. C. McCollum, B. C. Passenheim, and H. W. White, *Phys. Rev.* **161**, 652 (1967).
- ¹⁶W. DeSorbo, *Acta Metall.* **1**, 503 (1953).
- ¹⁷D. C. McCollum and W. A. Taylor, *Phys. Rev.* **156**, 782 (1967).
- ¹⁸H. K. Collan, M. Krusius, and G. R. Pickett, *Phys. Rev. B* **1**, 2888 (1970).
- ¹⁹K. G. Ramanathan and T. M. Srinivasan, *Phys. Rev.* **99**, 442 (1955).
- ²⁰I. N. Kalinina and P. G. Strelkov, *Sov. Phys. JETP* **7**, 426 (1958).
- ²¹The ABINIT code is a common project of the Université Catholique de Louvain, Corning Incorporated, and other contributors (<http://www.abinit.org>).
- ²²C. Hartwigsen, S. Goedecker, and J. Hutter, *Phys. Rev. B* **58**, 3641 (1998).
- ²³X. Gonze and C. Lee, *Phys. Rev. B* **55**, 10355 (1997).
- ²⁴X. Gonze, J.-M. Beuken, R. Caracas, F. Detraux, M. Fuchs, G.-M. Rignanese, L. Sindic, M. Verstraete, G. Zerah, F. Jollet *et al.*, *Comput. Mater. Sci.* **25**, 478 (2002).
- ²⁵X. Gonze, G.-M. Rignanese, and R. Caracas, *Z. Kristallogr. - New Cryst. Struct.* **220**, 458 (2005).
- ²⁶S. Goedecker, M. Teter, and J. Hutter, *Phys. Rev. B* **54**, 1703 (1996).
- ²⁷L. A. Hemstreet, C. Y. Fong, and J. S. Nelson, *Phys. Rev. B* **47**, 4238 (1993).
- ²⁸R. I. Sharp and E. Warming, *J. Phys. F: Met. Phys.* **1**, 570 (1971).
- ²⁹F. Herman and S. Skillman, *Atomic Structure Calculations* (Prentice-Hall, Englewood Cliffs, NJ, 1963).
- ³⁰J. Serrano, K. Syassen, A. H. Romero, A. Bosak, and M. Krisch (unpublished).